Production of Heavy Neutral MSSM Higgs Bosons a complete 1-loop calculation.

V. Driesen, W. Hollik and J. Rosiek*

Institut für Theoretische Physik, Universität Karlsruhe, D-76128 Karlsruhe, Germany

Abstract

The complete 1-loop diagrammatic calculations of the cross sections for the neutral Higgs production processes $e^+e^- \to Z^0H^0(Z^0h^0)$ and $e^+e^- \to A^0H^0(A^0h^0)$ in the MSSM are presented and compared the with the corresponding results of the simpler and compact effective potential approximation.

1. Introduction

In order to experimentally detect possible signals of the neutral MSSM Higgs bosons, detailed studies for the decay and production processes of Higgs boson are required. As has been discovered several years ago [1-3], radiative corrections in the MSSM Higgs sector are large and have to be taken into account for phenomenological studies. Three main approaches have been developed to calculate the 1-loop radiative corrections to the MSSM Higgs boson masses, production and decay rates:

a) The Effective Potential Approach (EPA) [2].

b) The Renormalization Group approach (RGE) [3].

c) The diagrammatic calculation in the on-shell renormalization scheme (Feynman Diagram Calculation, FDC) [4, 5]: The masses are calculated from the pole positions of the Higgs propagators, and the cross sections are obtained from the full set of 1-loop diagrams contributing to the amplitudes, including [4]:
   - the most general form of the MSSM lagrangian with soft breaking terms,
   - the virtual contributions from all the particles of the MSSM spectrum,
   - all 2-, 3- and 4-point Green's functions for a given process with Higgs particles,
   - the momentum dependence of the Green's functions,
   - the leading reducible diagrams of higher orders corrections.

The experimental searches for Higgs bosons at LEP1 [6] and studies for the future searches at higher energies [7] conventionally make use of the most compact effective potential approximation. We present the complete 1-loop diagrammatic results for the cross sections for the neutral Higgs production processes $e^+e^- \to Z^0H^0(Z^0h^0)$ and $e^+e^- \to A^0H^0(A^0h^0)$, compare them with the corresponding ones of the simpler and compact EPA approximation and discuss the typical size of the differences.

*Supported in part by the Alexander von Humboldt Stiftung and by the Polish Committee for Scientific Research.

2. Outline of the calculations

The tree level potential for the neutral MSSM Higgs bosons can be written as:

$$V^{(0)} = m_1^2 H_1^2 + m_2^2 H_2^2 + \epsilon_{ij}(m_{12}^2 H_1^i H_2^j + H.c.) + \frac{g^2 + g'^2}{8}(H_1^2 - H_2^2)^2 + \frac{g^2}{4}(H_1 H_2)^2 \quad (1)$$

Diagonalization of the mass matrices following from the potential (1) leads to three physical particles: two CP-even Higgs bosons H^0 , h^0 and one CP-odd Higgs boson A^0 , and defines their tree-level masses m_H , m_h and m_A , with $m_H > m_h$, and the mixing angles α, β. The way of calculating the radiative corrections in the EPA and FDC methods is briefly described as follows:

In the EPA, the tree level potential $V^{(0)}$ is improved by adding the 1-loop terms [2]:

$$V^{(1)}(Q^2) = V^{(0)}(Q^2) + \frac{1}{64\pi^2} \sum_{\substack{quarks \\ squarks}} \mathrm{Str}\mathcal{M}^4 \left(\log \frac{\mathcal{M}^2}{Q^2} - \frac{3}{2} \right) \quad (2)$$

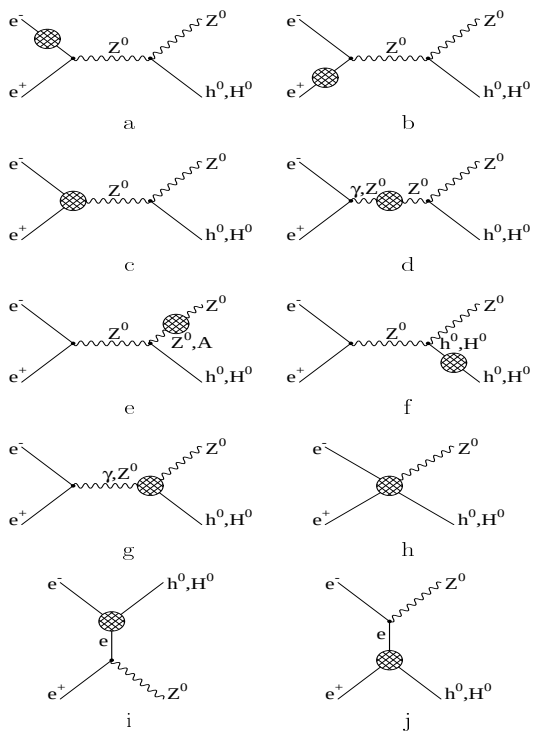

Figure 1: Classes of diagrams contributing to the $e^+e^- \to Z^0h^0(H^0)$ process in the FDC approach.

where $V^{(0)}(Q^2)$ is the tree level potential evaluated with couplings renormalized at the scale Q^2, and Str denotes the supertrace over the third generation of quark and squark fields contributing to the generalized mass matrix $\mathcal{M}^2$. The 1-loop potential $V^{(1)}$ is rediagonalized yielding the 1-loop corrected physical masses M_H , M_h and the effective mixing angle α_{eff} (for explicit formulae see [2]).

In the FDC the 1-loop physical Higgs boson masses are obtained as the pole positions of the dressed scalar propagators. M_H^2 and M_h^2 are given by the solution of the equation (3). For the calculations of the cross sections we need the full set of 2-, 3- and 4-point functions. In Fig. 1 the diagrams contributing to the $e^+e^- \to Z^0h^0(H^0)$ process are collected. The diagrams contributing to the $e^+e^- \to A^0h^0(H^0)$ process can be obtained by changing Z^0 into A^0 on the external line and skipping the diagrams i), j).

$$\mathrm{Re}\left[\left(p^2 - m_h^2 - \Sigma_{hh}(p^2)\right)\left(p^2 - m_H^2 - \Sigma_{HH}(p^2)\right) - \Sigma_{hH}^2(p^2)\right] = 0 \quad (3)$$

The formulae for the cross sections obtained in the FDC differ from the Born expressions, because not only the effective masses are corrected but also new form factors and momentum dependent effects are considered (see [4] for a detailed description).

3. Results on production cross sections

In this section we present the results for $Z^0H^0(Z^0h^0)$ and $A^0H^0(A^0h^0)$ production from the FDC and discuss the quality of simpler EPA approximation. In all figures we use as an example the set of parameters listed in Table 1. μ is the parameter describing the Higgs doublet mixing in the MSSM superpotential. M_2 denotes the SU(2) gaugino mass parameter. For the U(1) gaugino mass we use the value $M_1 = \frac{5}{3}\tan^2\theta_W M_2$, suggested by GUT constraints. M_{sq}, M_{sl}, A_t and A_b are the parameters entering the sfermion mass matrices (for the detailed expressions see e.g. [8]). For simplicity we assume a common value M_{sq} for all generations of squarks, and a common M_{sl} for sleptons.

Parameter	m_t	M_A	M_{sq}	M_{sl}	M_2	μ	$A_t = A_b$
Value (GeV)	175	200	1000	300	1000	500	1000

Table 1: Parameters used for the numerical analysis.

From the theoretical point of view, the most convenient parameters for the Higgs sector are the mass M_A of the CP-odd Higgs boson and the ratio $\tan\beta = \frac{v_2}{v_1}$. From the experimental point of view it is more natural to use, depending on the process considered, the masses M_h or M_H of the CP-even Higgs instead of the formal quantity $\tan\beta$.

As a first step, we apply the conventional M_A , $\tan\beta$ parameterization. Figs. 2 and 3 show the production cross sections for the processes $\sigma(e^+e^- \to Z^0h^0, A^0h^0)$ and $\sigma(e^+e^- \to Z^0H^0, A^0H^0)$ for $\sqrt{s}$ = 500 GeV. For the chosen set of parameters the numerical differences can reach 30% at $\sqrt{s}$ = 500 GeV. They become more important with

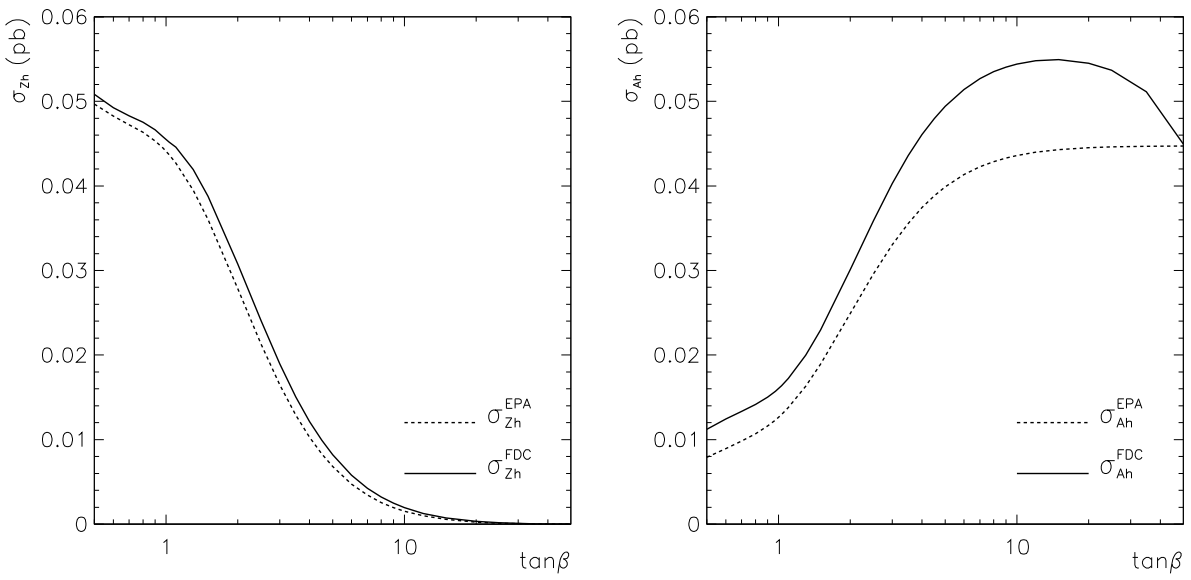

Figure 2: Comparison of the cross sections $\sigma(e^+e^- \to Z^0h^0, A^0h^0)$ obtained in the EPA and FDC. Parameters as given in Table 1, $\sqrt{s} = 500$ GeV.

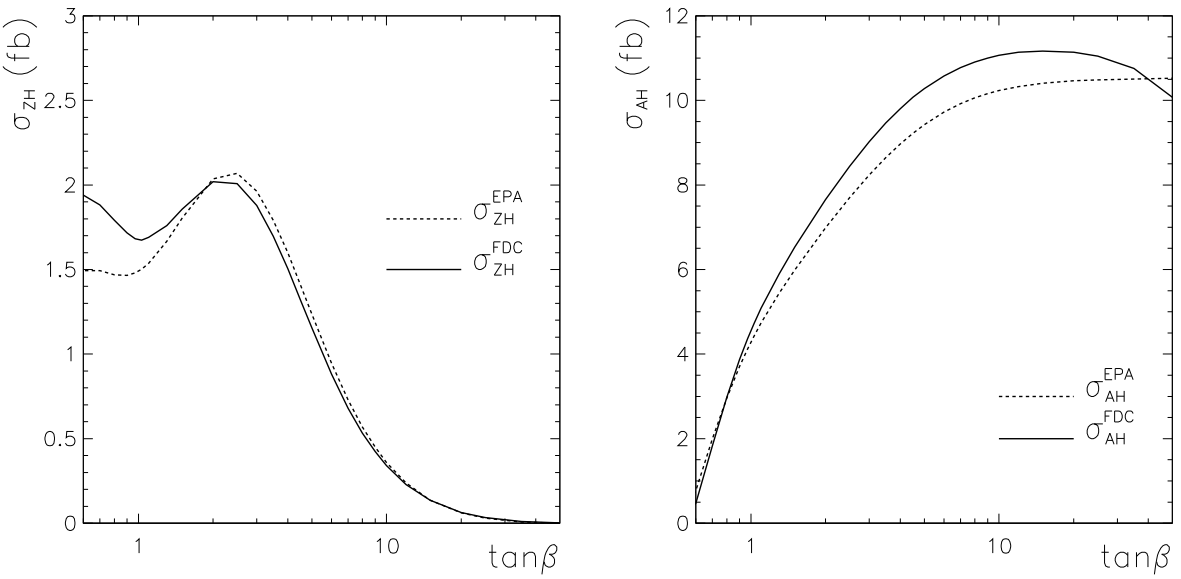

Figure 3: Comparison of the cross sections $\sigma(e^+e^- \to Z^0H^0, A^0H^0)$ obtained in the EPA and FDC. Parameters as given in Table 1, $\sqrt{s} = 500$ GeV.

increasing energies, exceeding 40% at 1 TeV. Note, however, that in the region of large cross sections the EPA accuracy is better (20% at 500 GeV). More detailed discussion of the lighter CP-even Higgs boson production can be found in ref. [9].

Fig. 4 shows the production cross sections for the processes $\sigma(e^+e^- \to Z^0H^0, A^0H^0)$ as a function of $\sqrt{s}$. The effect of the additional form factors included in the FDC grows when center-of-mass energy increases. For $\sqrt{s}$ = 1.5 TeV the differences between FDC and EPA can reach 50% for the $\sigma(e^+e^- \to Z^0H^0)$ production channel. In addition, the

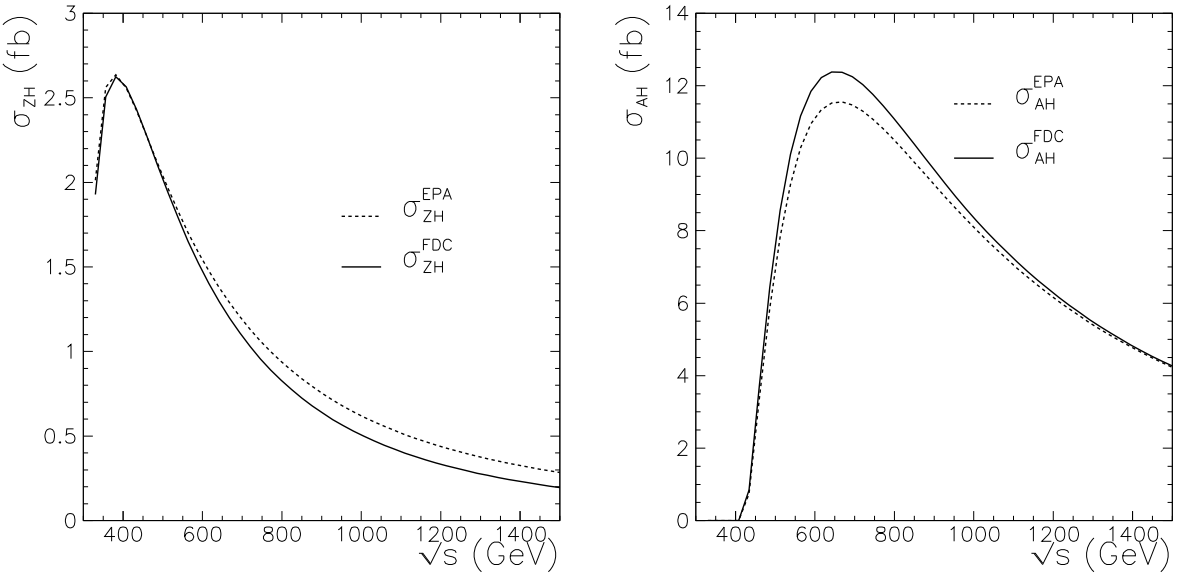

Figure 4: Comparison of the cross sections $\sigma(e^+e^- \to Z^0H^0, A^0H^0)$ as a function of $\sqrt{s}$ obtained in the EPA and FDC. $\tan\beta$ = 2, other parameters as given in Table 1.

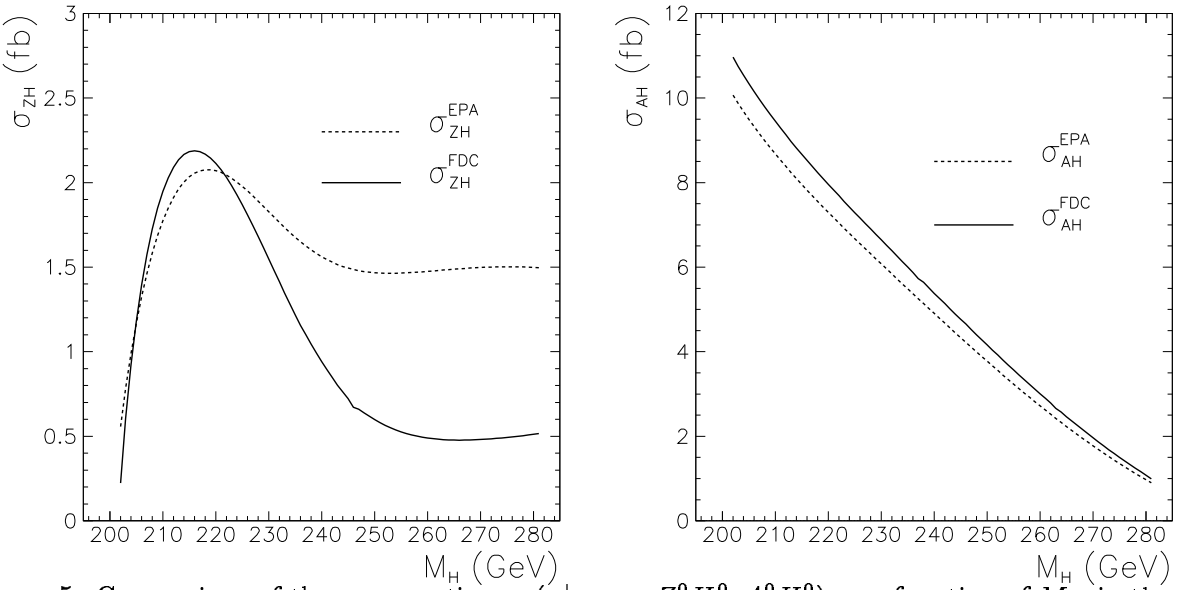

Figure 5: Comparison of the cross sections $\sigma(e^+e^- \to Z^0H^0, A^0H^0)$ as a function of M_H in the EPA and FDC. Parameters as given in Table 1, $\sqrt{s} = 500$ GeV.

angular dependence of the cross section given by the FDC is modified in compare to the effective Born approximation.

We now turn to the more physical parameterization of the cross sections in terms of the two Higgs boson masses M_A and M_h or M_H . This parameterization is more clumsy in the calculations, but it has the advantage of physically well defined input quantities avoiding possible confusions from different renormalization schemes. Varying M_H (M_A and other input quantities fixed) we obtain $\tan\beta$ and σ_{ZH}, σ_{AH} as functions of M_H . For the parameter values given in Table 1, the differences between the $\tan\beta$ values obtained in the EPA and FDC can reach 10% (up to 20% for smaller $M_A \approx 100$ GeV). Also significant differences can occur for the cross sections, as displayed in Fig. 5 where the predictions of EPA and FDC for the σ_{ZH} and σ_{AH} are plotted as functions of M_H . The typical size of differences between the methods is 10-20% for $\sqrt{s} = 500$ GeV, but they may became as large as 60% in case of the process $\sigma(e^+e^- \to Z^0H^0)$. This particularly large deviation occurs for large M_H values, corresponding to small $\tan\beta \leq 1$ (compare Fig. 2).

We have analyzed also the dependence of the differences between the EPA and the FDC predictions on the SUSY parameters: sfermion and gaugino masses, μ parameter and sfermion mixing parameters. In most cases the variation of those parameters does not have a large effect on the size of the differences between the EPA and FDC (a more detailed discussion can be found in ref. [10]).

To give a more global impression of the typical size of the differences between the EPA and FDC results, we have chosen 1000 random points (for each $\sqrt{s}$ value in Table 2) from the hypercube in the MSSM parameters space with the following bounds:

$0.5 < \tan\beta < 50$ | $50\ \text{GeV} < M_A < 250\ \text{GeV}$
-500 GeV $< \mu <$ 500 GeV | $200\ \text{GeV} < M_2 < 1000\ \text{GeV}$
$200\ \text{GeV} < M_{sq} = 2M_{sl} < 1000\ \text{GeV}$ | $-M_{sq} < A_t = A_b < M_{sq}$

We define the relative differences for the masses and cross sections as follows:

$$\delta X^{EPA} = \frac{X^{FDC} - X^{EPA}}{X^{FDC}}. \tag{4}$$

where X can be chosen as M_h , M_H , σ_{ZH}, σ_{Zh}, σ_{AH} or σ_{Ah}.

We calculated the quantities δM_h^{EPA}, δM_H^{EPA}, $\delta\sigma_{Zh}^{EPA}$, $\delta\sigma_{Ah}^{EPA}$, $\delta\sigma_{ZH}^{EPA}$and $\delta\sigma_{AH}^{EPA}$and averaged them (and also their absolute values) arithmetically over all generated points of the parameter space. The average mass differences are small and equal $|\delta M_h^{EPA}| = 2\%$ and $|\delta M_H^{EPA}| = 1\%$. The results for the cross sections are summarized in Table 2. It shows that the predictions of both methods deviate in particular for σ_{ZH}.

$\sqrt{s}$ (GeV)	$\delta\sigma_{Zh}^{EPA}$	$\delta\sigma_{Ah}^{EPA}$	$\delta\sigma_{ZH}^{EPA}$	$\delta\sigma_{AH}^{EPA}$	$\lvert\delta\sigma_{Zh}^{EPA}\rvert$	$\lvert\delta\sigma_{Ah}^{EPA}\rvert$	$\lvert\delta\sigma_{ZH}^{EPA}\rvert$	$\lvert\delta\sigma_{AH}^{EPA}\rvert$
500	16.4%	-2.4%	57%	4.4%	21%	31%	62%	14%
1000	10.3%	1.1%	56%	-3.0%	15%	31%	62%	14%
1500	4.2%	4.9%	53%	-9.0%	17%	32%	63%	18%

Table 2: Differences between the EPA and FDC predictions averaged over a random sample of parameters.

Summarizing, comparisons between the FDC predictions with the simpler EPA approximation have shown that at $\sqrt{s} = 500$ GeV the EPA has an accuracy of typically 10-20% in the parameter regions where the cross sections are large. The differences become larger with increasing energy, where also modifications of the Born-like angular distributions are more visible. The use of the physical input variables M_A, M_h or M_A, M_H avoids ambiguities from the definition of $\tan\beta$ in higher order, but the observed differences remain of the same size. For a better accuracy, the full FDC would be required.

Recently some papers on the leading 2-loop corrections to the CP-even MSSM Higgs boson masses have been published [11]. The main conclusion is that 2-loop corrections are also significant and tend to compensate partially the effects of 1-loop corrections. The calculations are based on the EPA and RG methods. Since the main emphasis of this study is to figure out the difference between complete and approximate results in a given order, we have not implemented the 2-loop terms. They would improve the 1-loop FDC results in the same way as the approximations and thus do not influence the remaining differences which can only be obtained by an explicit diagrammatic calculation.

The library of FORTRAN codes for the calculation of the 1-loop radiative corrections in the on-shell renormalization scheme to the MSSM neutral Higgs production and decay rates [4] can be found at the URL address:
http://itpaxp1.physik.uni-karlsruhe.de/~rosiek/neutral_higgs.html

References

1. S. P. Li, M. Sher, *Phys. Lett.* **B140** (1984), 339; J. Gunion, A. Turski, *Phys. Rev.* **D39** (1989) 2701; **D40** (1989) 2325, 2333; M. Berger, *Phys. Rev.* **D41** (1990) 225.
2. J. Ellis, G. Ridolfi, F. Zwirner, *Phys. Lett.* **262B** (1991) 477; R. Barbieri, M. Frigeni, *Phys. Lett.* **258B** (1991) 395; A. Brignole, J. Ellis, G. Ridolfi, F. Zwirner *Phys. Lett.* **271B** (1991) 123.
3. M. Carena, K. Sasaki, C.E.M. Wagner, *Nucl. Phys.* **381B** (1992) 66; H.E. Haber, R. Hempfling, *Phys. Rev.* **D48** (1993) 4280: P.H. Chankowski, S. Pokorski, J. Rosiek, *Phys. Lett.* **281B** (1992) 100.
4. P. Chankowski, S. Pokorski, J. Rosiek *Nucl. Phys.* **B423** (1994) 437; **B423** (1994) 497; V. Driesen, W. Hollik, *Z. Phys.* **C68** (1995) 485.
5. A. Brignole, *Phys. Lett.* **281B** (1992) 284.
6. ALEPH Collab., D. Buskulic et al., *Phys. Lett.* **313B** (1993), 312; DELPHI Collab., P. Abreu et al., *Nucl. Phys.* **373B** (1992), 3; L3 Collab., O. Adriani et al., *Z. Phys.* **57C** (1993), 355; OPAL Collab., R. Akers et al., Preprint CERN, PPE/94-104 (1994); J. F. Grivaz, Proc. of the International Europhysics Conference on High Energies, Brussels, July 27 - August 2, 1995; preprint LAL-95-83.
7. *Higgs Physics*, M. Carena, P. Zerwas et al., to appear in the Proceedings of LEP2 Workshop, CERN Yellow Report, eds. G. Altarelli et al.; *Higgs Particles*, in: e^+e^- Collisions at 500 GeV, DESY 92-123A,B,C, ed. P. Zerwas.
8. J. Rosiek, *Phys. Rev.* **D41** (1990) 3464; *erratum* hep-ph/9511250.
9. V. Driesen, W. Hollik, J. Rosiek, hep-ph/9512441, in print in *Z. Phys.* **C**.
10. J. Rosiek, A. Sopczak, *Phys. Lett.* **B341** (1994) 419.
11. R. Hempfling, A. Hoang, *Phys. Lett.* **B331** (1994) 99; M. Carena, J.R. Espinosa, M. Quiros, C.E.M. Wagner, *Phys. Lett.* **B355** (1995) 209; M. Carena, M. Quiros, C.E.M. Wagner, preprint CERN-TH-95-157, hep-ph/9508343.